Passivation and activation of $La_{0.6}Sr_{0.4}FeO_3$ thin film electrodes

Tripković, Dordije; Küngas, Rainer; Mogensen, Mogens Bjerg; Hendriksen, Peter Vang

Published in:
Physical Chemistry Chemical Physics

Link to article, DOI:
10.1039/d0cp02464c

Publication date:
2020

Document Version
Peer reviewed version

PCCP Physical Chemistry Chemical Physics Accepted Manuscript Passivation and activation of La 0.6 Sr 0.4 FeO 3 thin film electrodes

Article *in* Physical Chemistry Chemical Physics · June 2020

DOI: 10.1039/D0CP02464C

CITATION
1

READS
178

4 authors, including:

Đorđije Tripković
Karlsruhe Institute of Technology
18 PUBLICATIONS **61** CITATIONS

SEE PROFILE

Mogens Mogensen
Technical University of Denmark
403 PUBLICATIONS **20,961** CITATIONS

SEE PROFILE

Peter Vang Hendriksen
Technical University of Denmark
273 PUBLICATIONS **6,337** CITATIONS

SEE PROFILE

PCCP
Physical Chemistry Chemical Physics

Accepted Manuscript

This article can be cited before page numbers have been issued, to do this please use: . Tripkovi, R. Küngas, M. Mogensen and P. V. Hendriksen, *Phys. Chem. Chem. Phys.*, 2020, DOI: 10.1039/D0CP02464C.

View Article Online
DOI: 10.1039/D0CP02464C

Passivation and activation of $La_{0.6}Sr_{0.4}FeO_3$ thin film electrodes

Đorđije Tripković[1,], Rainer Küngas[2], Mogens Bjerg Mogensen[1], Peter Vang Hendriksen[1]*

[1] Department of Energy Conversion and Storage, Technical University of Denmark, Fysikvej Building 310, DK-2800 Kgs. Lyngby, Denmark

[2] Haldor Topsøe A/S, Haldor Topsøes Allé 1, Kgs. Lyngby, Denmark

Abstract

The oxygen exchange activity of thin dense $La_{0.6}Sr_{0.4}FeO_3$ electrodes prepared by pulsed laser deposition was investigated by electrochemical impedance spectroscopy and electrical conductivity relaxation below 600°C. The value of the surface exchange coefficient (k_{chem}) measured at 491°C decreased from initial $4.4 \cdot 10^{-6}$ cm/s to $1.7 \cdot 10^{-7}$ cm/s after aging for 7 days. The rapid decrease in the oxygen exchange rate was accompanied by the increase in the surface concentration of 'non-lattice strontium' detected by X-ray photoelectron spectroscopy. Subsequent electrochemical tests over 40 days showed that the electrode performance could be recovered by rinsing the passivated electrode in deionized water. Repeated treatments eventually also led to improved stability of electrochemical performance.

View Article Online
DOI: 10.1039/D0CP02464C

1. Introduction

Mixed ionic and electronic conductors (MIEC) are presently preferred oxygen electrode materials for solid oxide fuel and electrolysis cells (SOFC/SOEC). Apart from chemical stability and good mechanical compatibility with other cell components, one of the most important requirements for the electrode materials is high catalytic activity towards the oxygen reduction reaction (ORR). The ORR proceeds over several steps including adsorption, molecular dissociation, charge transfer, etc.[1,2] The exact mechanism of the reaction is still not fully understood and the rates of individual steps are usually not known. One can, however, measure the overall oxygen exchange rate at the surface (expressed through an appropriate rate constant k) using techniques such as isotope exchange (IE), electrical conductivity relaxation (ECR), and electrochemical impedance spectroscopy (EIS). Since the rate of surface oxygen exchange directly affects the electrochemical performance of technological MIEC electrodes, the determination of k of candidate electrode materials is important for SOFC/SOEC development.[3,4]

Recently, we have shown that the passivation of electrode materials over time may be due to an intrinsic property of the perovskite surface to reversibly crystallize in different phases at different temperatures.[5,6] As a continuation of these studies on bulk $La_{0.6}Sr_{0.4}FeO_3$, we here present results obtained on thin film model electrodes made by pulsed lased deposition of the same material. Due to their particular and simple geometry (well-defined surface, short bulk diffusion path), thin film electrodes are well-suited for characterization of oxygen exchange kinetics at the surface. Furthermore, their small volume and hence relatively fast relaxation times allows us to probe the kinetics at temperatures below 600°C, which is largely impractical in bulk samples.

The electrodes were tested by impedance spectroscopy over a period of 46 days with two surface treatments in deionized water introduced in an attempt to reactivate the surface.[7] The specific

View Article Online
DOI: 10.1039/D0CP02464C

thermal history of the samples coupled with surface analysis enables the elucidation of passivation and activation phenomena on the perovskite surface.

2. Experimental

The here investigated LSF thin film electrodes were prepared by pulsed laser deposition (PLD). PLD targets were prepared from commercial powders: $(La_{0.6}Sr_{0.4})_{0.99}FeO_{3-\delta}$ (Kusaka Rare Metal Products Co.Ltd., >99%) for the LSF target and $Ce_{0.9}Gd_{0.1}O_{1.95}$ (Solvay S.A., >99%) for the CGO target. The PLD targets were prepared using the same procedure as for the preparation of dense bars for electrical conductivity relaxation which is described in detail elsewhere.[5,6]

One-side polished, (100)-oriented, monocrystalline substrates of yttrium-stabilized zirconia (YSZ, 9.5 mol% Y_2O_3, CrysTec GmbH, Germany) with the size of 10 mm x 10 mm x 0.5 mm served as the electrolyte. Before the PLD deposition, a porous and 10 µm thick layer of platinum infiltrated with $Ce_{0.8}Pr_{0.2}O_{1.9}$ (CPO) was prepared on the non-polished 'backside' of the single crystal to serve as counter electrode for the electrochemical measurement. First, a paste consisting of small platinum flakes (Alfa Aesar, >99.9%) was brush-painted on the non-polished side of the substrate and calcined at 900°C for 2 hours with ramp rate of 2°C/min during heating and cooling. The formed porous layer of platinum was then infiltrated twice with a drop of 3M solution of CPO (mixture of Ce- and Pr-nitrates in 80:20 molar ratio) mixed with 3 wt% of surfactant Triton X100. After each infiltration, samples were calcined for 1 hour at 300°C. CPO was infiltrated in order to increase the performance of the counter electrode to a level where its contribution to the total impedance of the cell is negligible.[8]

The films were deposited on the polished surface using a KrF excimer laser (Surface systems+technology GmbH, Germany) of 248 nm wavelength with a fluence of 2.4 J/cm^2 measured at the target. The substrate temperature during all depositions was kept constant at

View Article Online
DOI: 10.1039/D0CP02464C

600°C. A physical mask was used during the deposition which reduced the total electrode area to 66±2 mm^2 (Figure S1-a). First, a buffer layer of CGO was deposited with 9000 laser pulses (ν = 5 Hz) in a small oxygen flow realizing pressure of 0.001 mbar. On top of that, a layer of LSF was deposited with 10^5 pulses (ν = 10 Hz) in a flow of oxygen at 0.03 mbar. Four cells were prepared using the described procedure (2 were used for EIS measurements and surface analysis, 1 for ECR, and 1 for SEM, XRD, and profilometry). The samples were cooled down in the chamber under the same gas activity as applied during film deposition. After the deposition, the samples were kept in closed containers protecting the surface mechanically and from contamination, but containers were not gas-tight.

The crystallinity of the deposited thin film was analyzed by XRD using a Rigaku Smartlab (Figure S2). The surface and cross section of the electrodes were also examined by scanning electron microscopy (SEM), Zeiss Merlin microscope. The total electrode thickness was found to be approximately 255±5 nm based on SEM cross section and thickness measurement by a Dektak stylus profiler (Figure S3).

Electrochemical impedance spectroscopy (EIS) was carried out in a rig made of alumina (Figure S1-b). The electrodes were contacted by sandwiching the cells between two current collectors made of woven gold meshes (wire thickness 80 µm, aperture of 250 µm, purity >99.9%) wrapped around CGO pellets. A small mechanical force (≈ 10 kPa) was applied to ensure the contact. Before the test, all rig elements were acid cleaned in concentrated HCl and deionized water. The cells were tested in dry O_2/N_2 gas mixtures with a flow of 5 l/h and pO_2 was varied in the range from 1 to 0.05 mbar. The realized oxygen activity was measured by a zirconia-based oxygen sensor placed on the exhaust stream. The temperature was measured by a thermocouple placed close to the cell (within 2 mm). The impedance was measured at 48 different frequencies in the frequency range

View Article Online
DOI: 10.1039/D0CP02464C

from 10^5 to 10^{-1} Hz with no DC current applied. A Solartron 1260 frequency response analyzer was used and the applied signal amplitude was 10 mV. Logging and parameter fitting was done by an in-house developed software Elchemea. An overview of electrochemical testing can be found in Figure 1 which shows experimental parameters (temperature and pO_2) plotted versus t_{exp} which represents the time since the start of the experiment The performance was first tested at 11 different temperatures from 387°C to 594°C (Arrhenius test). The reported oxygen exchange and R_{ORR} values are averages of three consecutive measurements on two identical cells at each temperature. The error bars were smaller than the symbols and hence are not shown in the plots. After the temperature dependence test, the performance of the electrodes was tested at different pO_2 from 1 to 0.05 bar at 491°C (pO_2 test). Finally, the electrochemical stability was tested over 60 hours in pure oxygen (pO_2=1 bar) at 491°C (stability test). After this step, the electrodes were cooled down to room temperature in oxygen with a ramp rate of 3°C/min. One sample was then taken out for the surface analysis ('aged' sample) while the other was rinsed in deionized water for 5 min at 50°C, reinserted in the rig, heated up to 491°C with a ramp rate of 2°C/min and the stability test continued for 3 weeks. The electrode was then subjected to another treatment in water and its performance was tracked for another 2 weeks. Finally, the electrode was cooled down in oxygen at a ramp rate of 3°C/min and without any further treatments taken to surface analysis ('rinsed' sample). The surface of the electrodes was analyzed by XPS using Physical Electronics Versaprobe II X-ray Photoelectron Spectrometer with monochromated Al Kα (1486.65 eV) X-ray radiation source equipped with charge neutralization system under a base pressure of 10^{-9} Torr. In total, three XPS measurements were done including survey scans and detailed scans focusing on the Sr *3d* peak:

1) 'as deposited' - immediately after the PLD;

View Article Online
DOI: 10.1039/D0CP02464C

2) 'aged' - after 7 days of electrochemical testing and before the first rinsing;

3) 'rinsed' - after the long-term test (46 days) which involved two treatments in water;

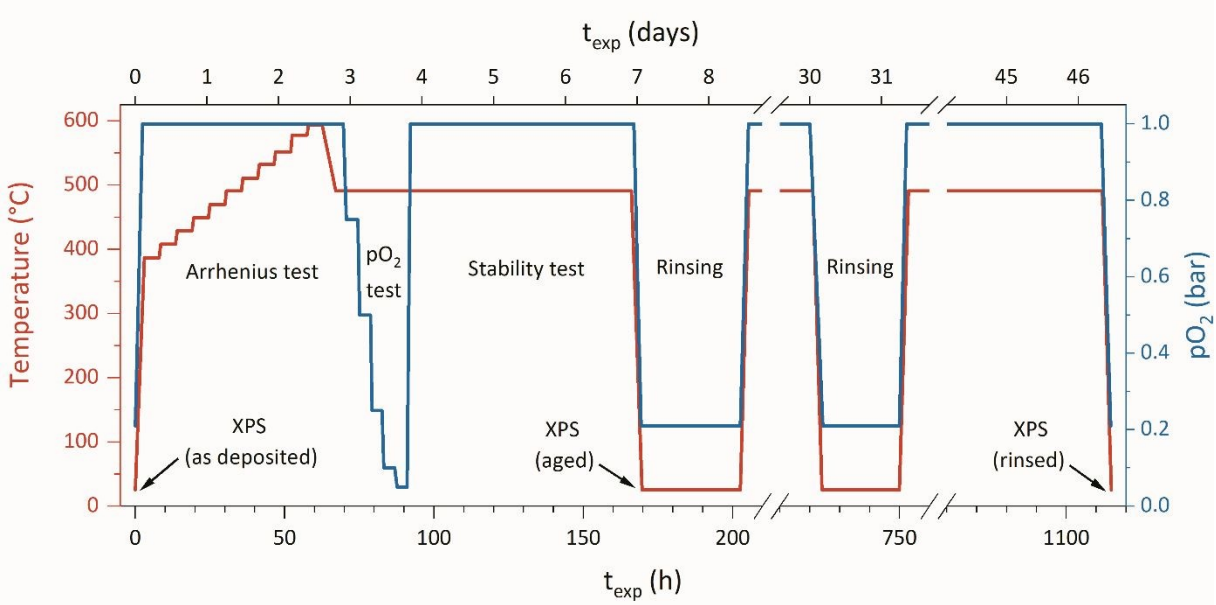

Figure 1. Experimental conditions (temperature and oxygen partial pressure) during electrochemical characterization. t_{exp} stands for the time since the start of the experiment and is indicated in the subsequent figures for easier reference to thermal history. Three XPS analyses shown in Figure 6 are carried out at the points indicated by arrows.

Another thin film LSF electrode was characterized by ECR in order to test the validity of k_{chem} values obtained by EIS. The electrode was connected to a four probe measurement setup with high-purity platinum wires (99.99%). The contact was ensured by applying a small amount of platinum paste (Ferro, 99.2%). The ECR experiment was conducted in a sealed quartz-tube reactor of approximately 10 ml in volume. The total gas flow was kept constant at 5 ml/s and the change in conductivity was measured after imposing an abrupt change in pO_2 from 0.2 to 0.1 bar. The temperature was measured by a thermocouple placed 1 mm above the electrode surface, and pO_2 was measured by a zirconia sensor exposed to the exhaust stream. The relevant parameters were logged with a sampling rate of 1 Hz. Fitting and parameter extraction was done in *ECReX*.[5] The experimental setup for the ECR of the thin films is shown in Figure S1-c.

View Article Online
DOI: 10.1039/D0CP02464C

3. Results

3.1. Impedance spectroscopy

The area specific resistances measured during the first heating run are shown in Figure 2 along with results for several other model electrodes from the literature. The area specific resistance is calculated with ($ASR_{norm} = R_{ORR} \cdot A_{act.}$) and without area normalization ($ASR = R_{ORR} \cdot A_{geom.}$) where $A_{act.}$ stands for the calculated active electrode area based on the electrolyte resistance and $A_{geom.}$ stands for the geometrical area of the electrode (66±2 mm^2). More details about the normalization can be found in the supplementary information. Since $A_{geom.}/A_{act.} \approx 2$, the difference between the calculated ASR values is $ASR/ASR_{norm.} \approx 2$. The apparent activation energy associated with the ASR was found to be 1.45±0.03 eV (≈140 kJ/mol). After the pO_2 test and additional 60 hours at 491°C (t_{exp} = 170h), the ASR increases 37x (indicated by an arrow). Inspection of the literature values from several thin film studies reveals that results fall in three groups which do not seem to depend strongly on the composition of the thin film electrode. The ASR obtained in this study follows a trend similar to that reported for $Ba_{0.5}Sr_{0.5}Co_{0.2}Fe_{0.8}O_3$ (Baumann et al.[9]), $La_{0.6}Sr_{0.4}CoO_3$ (Adler et al.[10] and Januschewsky et al.[11]), $La_{0.6}Sr_{0.4}Co_{0.2}Fe_{0.8}O_3$ (Darbandi et al.[12]), and the behavior of vertically aligned nanocomposite of Ruddlesden-Popper/perovskite $LaSrCoO_4/La_{0.8}Sr_{0.2}CoO_3$ reported by Ma et al.[13]. A clear outlier is the measurement by Crumlin et al.[14] for $La_{0.8}Sr_{0.2}CoO_3$ electrode modified with a small amount of $LaSrCoO_4$. The observed fast kinetics in that study was attributed to the presence of fast Ruddlesden-Popper/perovskite interfaces. The same phenomenon is credited for fast kinetics in case of multiphase "$La_{0.6}Sr_{0.4}CoO_3$" reported by Hayd et al.[15], yet the electrode was not fully dense (meaning that $A_{act.} > A_{geom.}$). On the other hand, ASR values reported by Plonczak et al.[16] for $La_{0.6}Sr_{0.4}Co_{0.2}Fe_{0.8}O_3$ and by Baumann et al.[9] for $La_{0.6}Sr_{0.4}FeO_3$ were 2-3 order of magnitude higher than in the present

View Article Online
DOI: 10.1039/D0CP02464C

study. In the case of Plonczak et al.[16] the high values of ASR are likely a consequence of the use of a platinum paste for current collection. The paste has later been shown to be detrimental for oxygen exchange kinetics[17], likely due to the presence of impurities in the paste. Furthermore, the ASR values reported by Plonzcak et al. refer to the electrode performance after aging at 750°C for 42h which was done to ensure reproducibility (the performance, albeit reduced, was more stable after aging).[16]

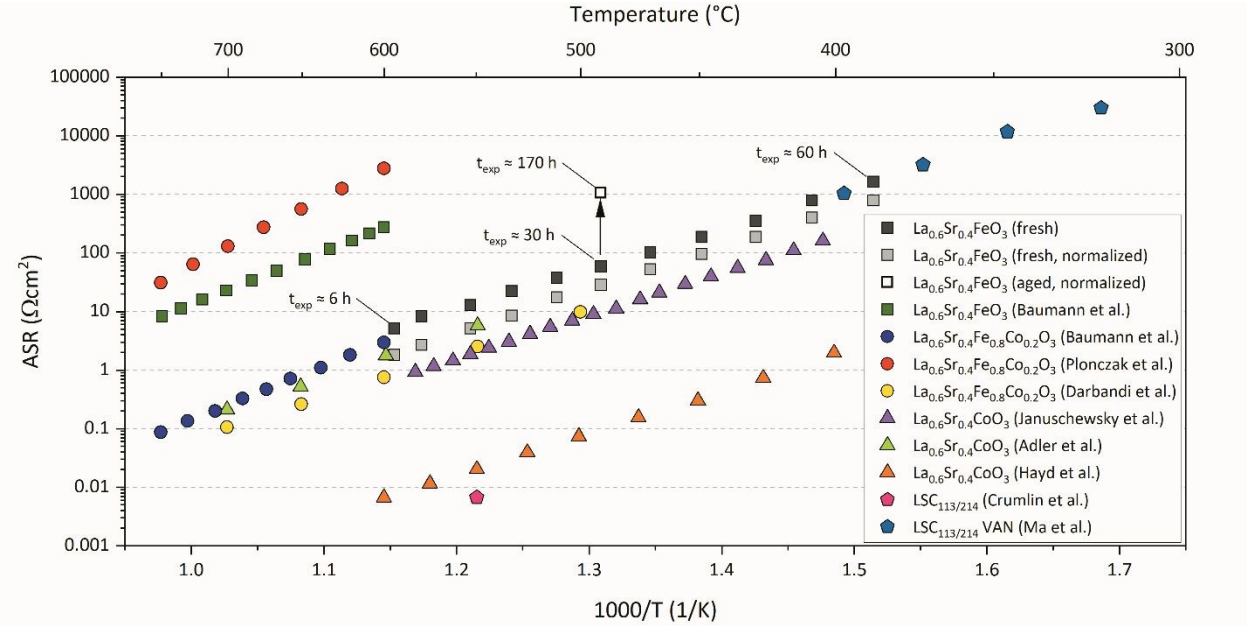

Figure 2. Temperature dependence of area specific resistances calculated with ($ASR_{norm} = R_{ORR} \cdot A_{act}$) and without normalization ($ASR = R_{ORR} \cdot A_{LSF}$) and the selected literature values.[9–16] Arrow indicates the change from the initial ASR value measured at 491°C and pO_2 = 1 bar (designated as 'fresh', measured at approximately 30 hours since the start of the experiment) to the one measured 140 hours later at the same conditions (designated as 'aged', approximately 170 hours since the start of the experiment).

The significant scattering of the reported ASR values illustrates the importance of factors other than the material composition for the performance of thin film electrodes. The fact that these discrepancies are usually much larger in thin films (where $A_{act} \sim A_{geom}$) when compared to bulk and

View Article Online
DOI: 10.1039/D0CP02464C

technological electrodes (where $A_{act.} >> A_{geom.}$) suggests that the surface-related phenomena play the crucial role.

Using the acquired impedance spectra at different temperatures (T = 387-594°C, pO_2 = 1 bar) and a subsequent measurements at different oxygen partial pressures (T = 491°C, pO_2 = 0.05-1 bar) we calculated corresponding oxygen exchange coefficients k_O and k_{chem} using the following equations:

$$k_{chem} = 2\pi f_{summit} \cdot L \qquad (Eq.\ 1)$$

$$k_O = \frac{RT}{n^2 F^2 A C_O} \cdot \frac{1}{R_{ORR}} \qquad (Eq.\ 2)$$

In the equations above, f_{summit} stands for the summit frequency of the ORR semicircle, R is the universal gas constant, T is temperature, n is the charge of the diffusing ion (-2 for oxygen), F is Faraday's constant, A is the electrode area, C_O is the concentration of oxygen ions in the lattice, and R_{ORR} is the surface resistance due to oxygen exchange reaction. More about the derivation of Eq.1 and Eq.2 can be found in the supplementary information.

Oxygen exchange values at different temperature and pO_2 are shown in Figure 3. Both k_{chem} and k_O are found to be strongly temperature-dependent with activation energy of 146.6 kJ/mol in case of k_O and 129.4 kJ/mol in case of k_{chem}. The partial pressure of oxygen also affects the oxygen exchange coefficients. The observed pO_2 dependence can be well described by a power law relation ($k \sim pO_2^n$), which in log-log plot shown in Figure 3 gives a straight line. The exponent n is in both cases found to be close to ½, which indicates that the rate determining step involves singular oxygen species.[2]

View Article Online
DOI: 10.1039/D0CP02464C

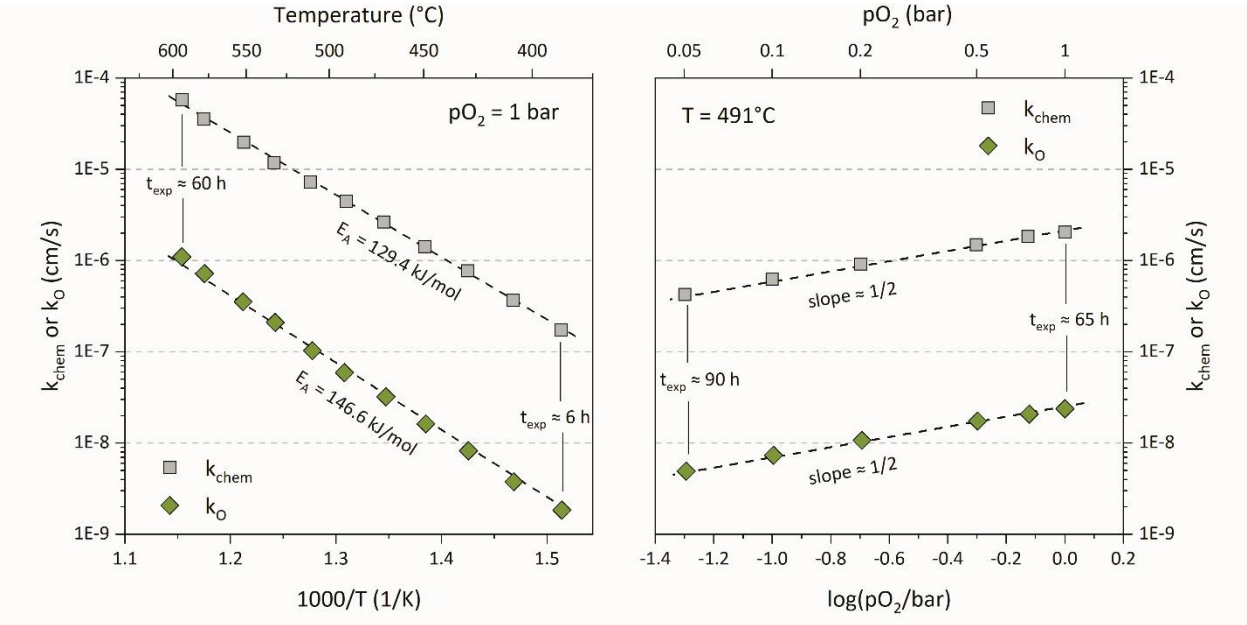

Figure 3. Values of oxygen exchange coefficients (k_{chem} and k_O) calculated from impedance spectroscopy data using the equations Eq.1 and Eq.2. Left) Oxygen exchange coefficients between 387 and 594°C at pO_2 = 1 bar based on impedance measurements collected between t_{exp} = 6 h and t_{exp} = 60 h. Right) Oxygen exchange coefficients in pO_2 range between 0.05 and 1 bar at 491°C based on measurements performed between t_{exp} = 65 h and t_{exp} = 90 h.

3.2. Electrical conductivity relaxation

The oxygen exchange kinetics of the prepared thin film electrodes was also measured by ECR. Due to thin film geometry and surface-controlled kinetics, we can use the following equation for calculating k_{chem}:

$$\frac{\sigma(t)-\sigma_\infty}{\sigma_0-\sigma_\infty} = exp\left(\frac{-k_{chem}\cdot t}{L}\right) \quad (Eq.3)$$

where σ,σ_0, and σ_∞ stand for electrical conductivity at the time t and L is film thickness. A comparison between ECR-measured k_{chem} values and the ones based on the impedance measurements (calculated using Eq. 1) can be found in Figure 4. ECR analysis in the ideal case requires instantaneous pO_2 change. This requirement can be fulfilled when the time needed for flushing the reactor is more than 20 times smaller than the time constant of the measured

View Article Online
DOI: 10.1039/D0CP02464C

process.[18] Due to small volume, thin film electrodes equilibrate very fast, which needs to be compensated either by short flushing time (high gas flow rates, small reactor volume) or by performing measurements in an experimental region where the reaction kinetics are slower (low temperature and pO_2). Since there were practical limitations to the former, the ECR analysis could be performed only below 430°C and in pO_2 lower than 0.2 bar. Therefore, in contrast to the EIS study, ECR-derived k_{chem} values were obtained at pO_2=0.1 bar (end pO_2). It can be concluded that the k_{chem} values obtained by two different techniques match very well when the difference in pO_2 is taken into account. This finding is important to show the possibility of obtaining k_{chem} values from the impedance measurement of thin dense films, a procedure that is rarely used in the literature despite the fact that it requires no additional experiments.

Literature values obtained on thin film and bulk electrodes of the same composition are also shown in Figure 4. A large part of the scatter between the literature values can be ascribed to different thermal history, which has been discussed in a previous study carried out on bulk-type samples.[5] In that study, it was shown that k_{chem} values can vary greatly (more than a factor of 60 at 650°C) and in a reproducible manner depending on the thermal history of the sample. Furthermore, this phenomenon was found to be strongly correlated to the formation of inactive Sr-phases on the sample surface.[6] Figure 4 shows the k_{chem} trends (and extrapolations to lower temperatures) associated with the 'activated' and 'passive' state of LSF found in bulk studies. The k_{chem} values obtained in this study in the initial heating run(t_{exp} = 6 – 60 h) for thin film electrodes lie between the extrapolated values of 'passive' and 'activated' state found in bulk LSF, although somewhat closer to the latter. After 7 days of electrochemical testing, the thin film electrode deteriorates and the k_{chem} value drops more than two orders of magnitude (t_{exp} = 170 h). Remarkably, the new k_{chem} value falls exactly on the extrapolated line from the 'passive' state. Hence, a similar type of

View Article Online
DOI: 10.1039/D0CP02464C

passivation, likely ascribable to the same phenomenon (Sr enrichment and phase transformation), appears to take place in the thin film electrodes.

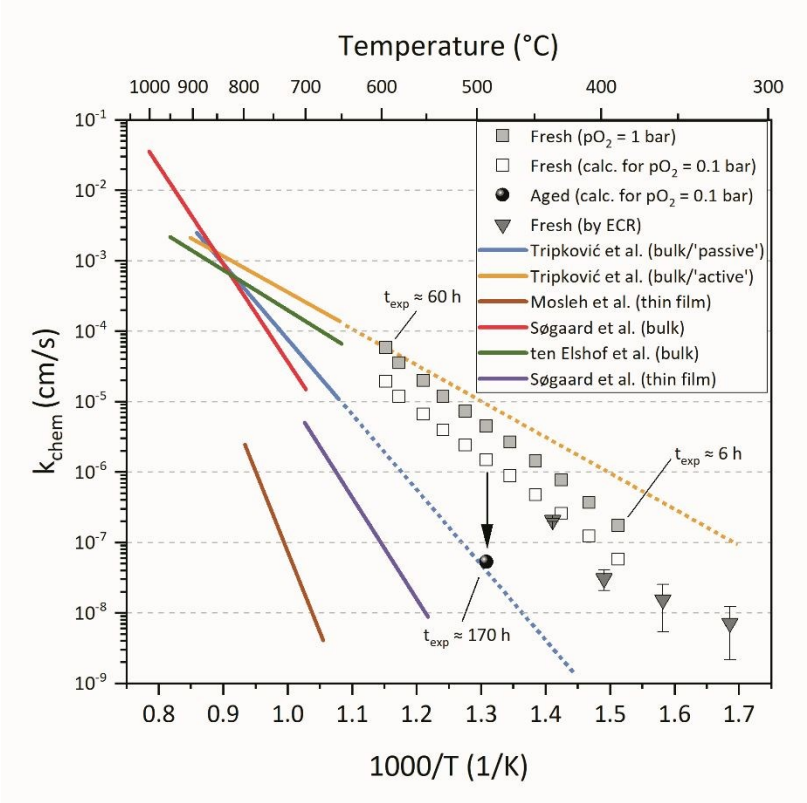

Figure 4. Comparison of oxygen exchange coefficient (k_{chem}) obtained in this study by impedance spectroscopy (using Eq. 1) and by electrical conductivity relaxation (using Eq. 3) along with values from the literature[2,5,19–21] 'Fresh' refers to the EIS measurement during the initial heating run (t_{exp} = 6-60 h). 'Aged' is the k_{chem} value obtained after 7 days of electrochemical testing (t_{exp} = 170 h). Since ECR and EIS measurements are performed under different pO_2, the k_{chem} values are calculated for the same oxygen activities based on the pO_2 dependence of ½ shown in Figure 3. 'Active' and 'passive' state refers to findings from the earlier study on bulk LSF by ECR.[5] Dotted parts are extrapolations to lower temperatures.

In the aforementioned bulk studies[5,6] it was also shown that the samples could be reversibly cycled between the two states by a high temperature thermal treatment, which was observed also to lead to a dissolution (or disappearance) of the Sr-rich phase that impedes surface exchange and re-formation of an active perovskite or Ruddlesden-Popper-like surface. Assuming that a similar

View Article Online
DOI: 10.1039/D0CP02464C

degradation mechanism is taking place in the thin film electrodes, we attempted to recover the initial performance by dissolving the anticipated passivating Sr-rich layer in deionized water (Figure 5). After aging for 3 days in oxygen at 491°C (t_{exp} = 170 h), k_{chem} decreased to $1.7 \cdot 10^{-7}$ cm/s. The samples were cooled down to room temperature and one was rinsed in deionized water (the other was used for XPS analysis). Upon heating up, the measured k_{chem} was $1.2 \cdot 10^{-6}$ cm/s (≈7x higher than before the treatment). The sample was then aged for 7 days, during which k_{chem} decreased again, reaching $\approx 1.2 \cdot 10^{-8}$ cm/s (100x lower than after the rinsing and 360x lower than in the initial measurement at t_{exp} = 30 h). Further aging for 10 days did not lead to any further deterioration indicating that the electrode was fully passivated, but retained a certain oxygen exchange activity. A second rinsing cycle led to k_{chem} values identical to the values after the first rinsing, which indicates that the rinsing effectively brings the surface back to a state close to the pristine one. In addition, after the second rinsing, the deterioration was much slower, and after aging for 10 days, k_{chem} had decreased only 30 % from $1.2 \cdot 10^{-6}$ cm/s to $0.8 \cdot 10^{-6}$ cm/s. This is a surprising result that has not been observed in similar studies. For instance, Cai et al.[22] observed even slightly faster degradation rates after etching $La_{0.6}Sr_{0.4}CoO_3$ in HCl, which was observed to benefit exchange rates initially. However, one needs to bear in mind these studies were rather short-term, lasting typically 3 days, whereas in the present study the performance was tracked over several weeks. It is noteworthy that C_{chem} values remain constant during the test indicating that the electrode volume does not change (Figure 5), i.e. substantial chemical etching of the electrode bulk can be excluded. Hence, the changes in performance are not related to a change in surface area but must be related to the state and/or composition of the surface.

View Article Online
DOI: 10.1039/D0CP02464C

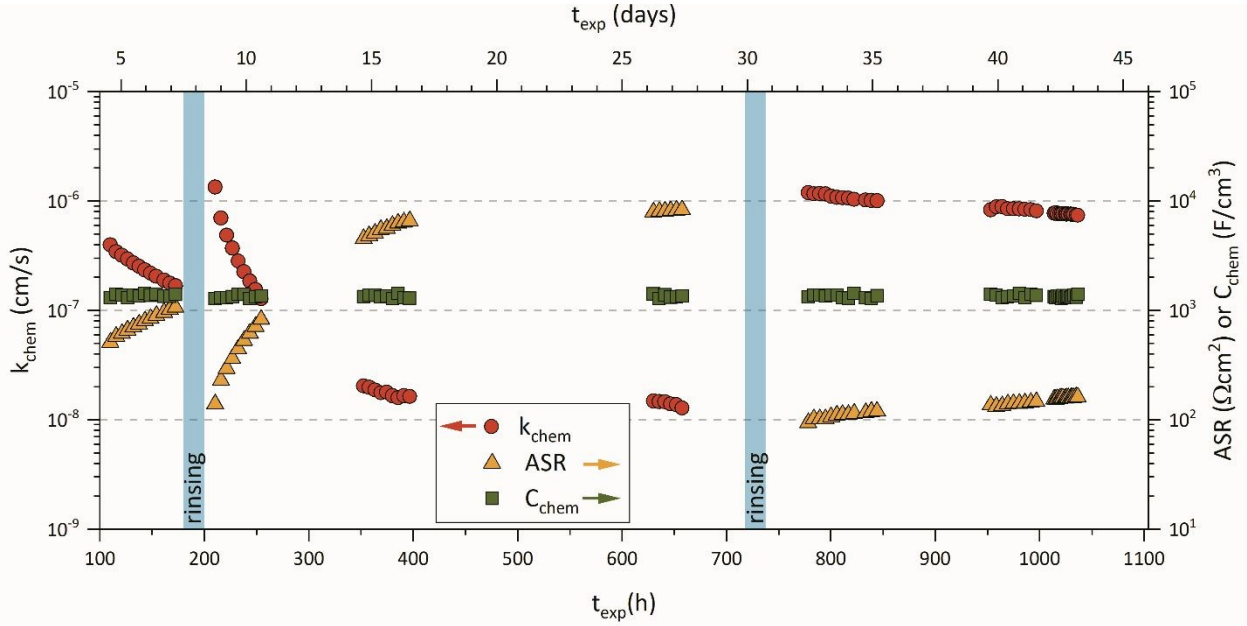

Figure 5. Long-term stability at 491°C and pure oxygen of LSF thin film electrode with intermittent rinsing in water. Surface exchange coefficient (k_{chem}, left axis), area specific resistance (ASR, right axis), and chemical capacitance (C_{chem}, right axis) are plotted against t_{exp}. The blue regions indicate the time when the rinsing in deionized water for 5 min at 50°C is performed but also account for the time needed for cool-down/heat-up of the rig.

3.3. Surface analysis

The chemical composition of the sample surface was investigated by XPS and the results are shown in Figure 6. The spectra are taken at different points in time during the experiment (Figure 1). The electrode was analyzed immediately after the PLD ('as deposited electrode', $t_{exp} = 0$), after 7 days of testing and before the first rinsing ('aged electrode', $t_{exp} = 170$ h), and finally after the whole long-term test and two treatments in water ('rinsed electrode', $t_{exp} = 1115$ h). Survey spectra (Figure 6-a) show the presence of the expected elements; La, Sr, Fe, and O from the electrode and C which inevitably forms when samples are exposed to atmospheric air.[6] No significant differences could be observed based on the survey spectra. This indicates that the degradation is not a consequence of poisoning with some detrimental elements such as chromium, sulfur, or silicon.

View Article Online
DOI: 10.1039/D0CP02464C

In addition to the survey spectra, detailed scans of the Sr *3d* peak were taken in order to further investigate the origin of electrode degradation (Figure 6-b). Due to orbital splitting, Sr *3d* peak comes in pairs of Sr $3d_{5/2}$ and Sr $3d_{3/2}$ peaks with the area ratio between them of 3:2 and a fixed energy separation of 1.7 eV. The observed Sr *3d* peaks could be fitted with two such doublets, labeled here as 'high energy Sr' (130.2±0.3 eV) and 'low energy Sr' (128.8±0.2 eV). Such a distinction between two states of Sr has also been observed in many other studies of Sr containing perovskite films.[22–26] The high energy component is usually suggested to be associated with Sr in form of secondary phases or in the outermost layers of the perovskite surface, while low energy component is related to strontium in the perovskite lattice. For these reasons, the two components are sometimes designated as 'surface Sr' and 'lattice Sr'.

The 'as deposited' thin film electrode had identical amounts of high and low energy Sr, similar to 'activated' state found in earlier studies.[5,6] A slightly higher amount of high-energy Sr was found on the surface after aging, which was accompanied by a loss in performance. Rinsed electrodes which had high oxygen exchange activity and stability had, in contrast, much less high energy component of Sr (only 22%).

View Article Online
DOI: 10.1039/D0CP02464C

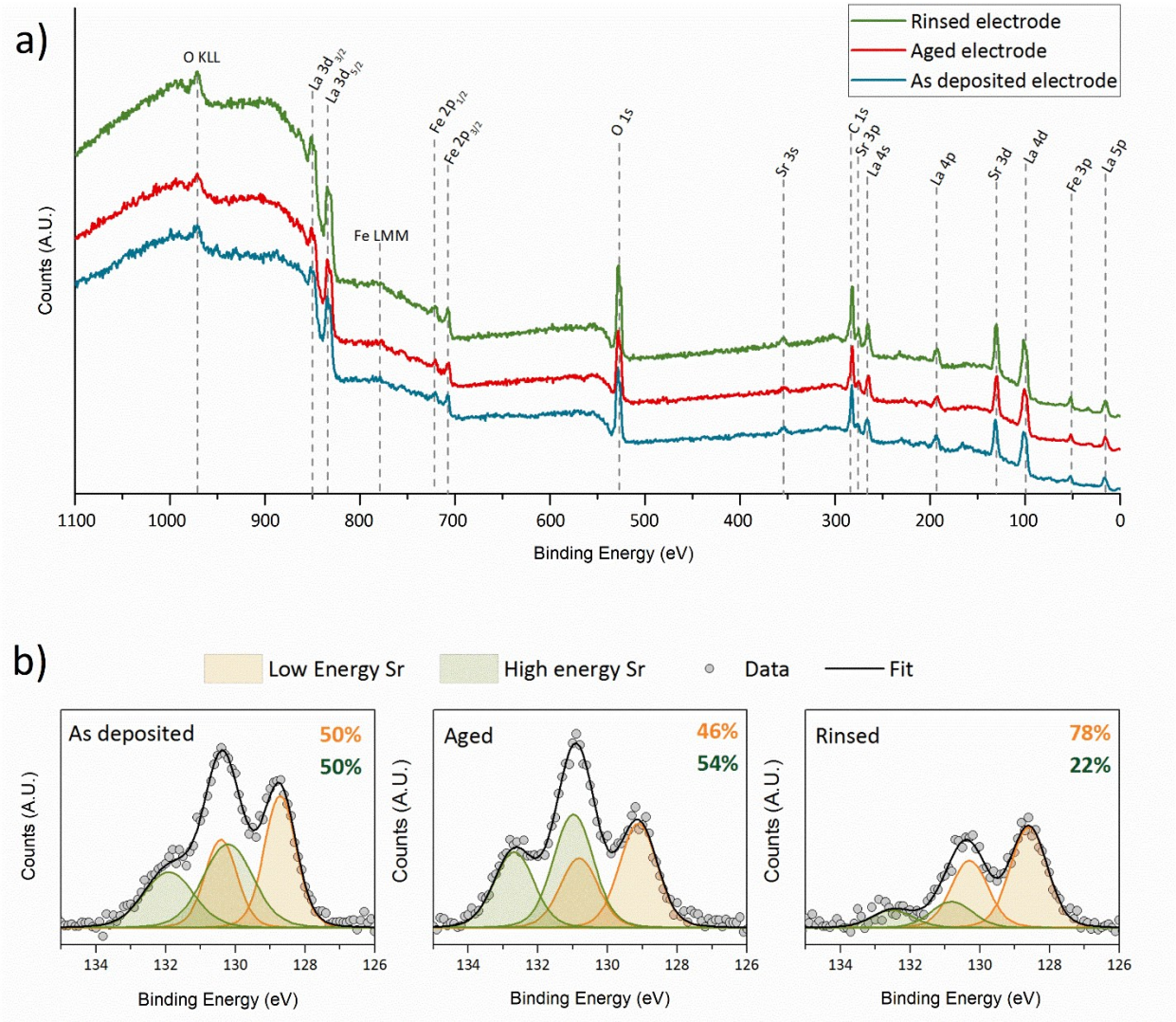

Figure 6. a) Survey XPS scans of the electrodes surface immediately after the PLD deposition (As deposited), after 7 days of electrochemical testing (Aged), and after 46 days of electrochemical testing and two rinsing treatments (Rinsed); b) Detailed XPS scans of Sr *3d* peak of LSF thin film electrode taken at different points in the experiment (see Figure 1) Relative content of each component in percentages is given in the corresponding color.

4. Discussion

Loss of oxygen exchange activity of perovskite electrodes is widely reported and has in many studies been ascribed to an observed Sr segregation.[22,27–30] In our previous study on bulk LSF electrodes, we have observed a strong correlation between the oxygen exchange performance and

View Article Online
DOI: 10.1039/D0CP02464C

the two states of Sr on the surface.[6] There, the samples with fast oxygen exchange kinetics ('activated' state) had almost the same amounts of high and low energy Sr components, while the overall Sr amount was found to be higher than nominal for the perovskite composition. After prolonged aging, k_{chem} values decreased to stable but much lower values ('passive' state). This was accompanied by an increase in the high energy Sr component to ≈60%. A correlation between the increase in high energy Sr component and loss of oxygen exchange activity has also been reported for $La_{0.6}Sr_{0.4}CoO_3$ electrodes implying that the phenomenon is general to several perovskites.[22] Furthermore, the transition was shown to follow Avrami-type kinetics which is characteristic for nucleation and growth processes[5] indicating that the change in the observed ratio between high and low energy Sr is caused by a change in phase composition at the surface. In other words, each Sr-containing phase presumably has a distinct XPS fingerprint depending on the local bonding environment of Sr and therefore, the change in high to low energy Sr ratio involves a phase transformation.

The same degradation mechanism seems to be responsible for the performance loss of the thin film electrode studied here. There is a clear analogy to the transition from 'activated' to 'passive' state that was found on the bulk samples.[5] Here, 'as deposited' electrode starts with identical amounts of high and low energy Sr and high oxygen exchange coefficients. The performance then gradually diminishes during the thermal treatment which is accompanied by an increase in the relative content of high energy Sr to 54%. Whereas the low energy strontium is consistently referred to Sr in the lattice, the origin of the high energy Sr remains elusive and has been ascribed to various phases such as SrO, spinels, brownmillerites, etc.[26,31] Noteworthy is the observation by Konysheva and Kuznetsov[31] that samples with higher amount of Ruddlesden-Popper phase had more low-energy Sr ('lattice Sr'). This suggests that the well-performing 'rinsed' surface

View Article Online
DOI: 10.1039/D0CP02464C

resembles a Ruddlesden-Popper phase, as opposed to the 'aged' surface which had low electrochemical activity, more high energy Sr, and is thus likely covered with detrimental Sr-rich phases.

Another similarity with bulk electrodes is the ability to recover the performance after the electrode reaches the passive state. In the bulk electrodes, this was accomplished by a thermal treatment at 1000°C which causes the secondary phases to re-dissolve in the perovskite (or first to decompose and remaining Sr to re-dissolve).[6] Here, instead of dissolution in perovskite lattice, the recovery of the oxygen exchange activity is accomplished by dissolving some or all of the exchange impeding Sr-rich phases in water as was also previously shown in the studies by Rupp et al.[7,29,30]

Following this line of thought, we can also attempt to explain the slower degradation rates observed after the second rinsing. A certain amount of strontium gets permanently removed from the electrode with each treatment in water, which markedly depletes the total amount of strontium due to small electrode volume. Eventually, this can cause less driving force for Sr segregation. The energy penalty for forming additional A-site vacancies in the bulk of the film electrode (as a consequence of the leaching of the Sr), reduces the energy gain by further "Sr-exsolution" at the surface). This reasoning is supported by XPS results where a very small relative content of high energy strontium was found in the rinsed electrode (only 22%). Such a low amount of high energy Sr is even more remarkable considering the fact that the electrode had spent additional 2 weeks at 491°C after rinsing. A sketch of the proposed mechanism is shown in Figure 7.

View Article Online
DOI: 10.1039/D0CP02464C

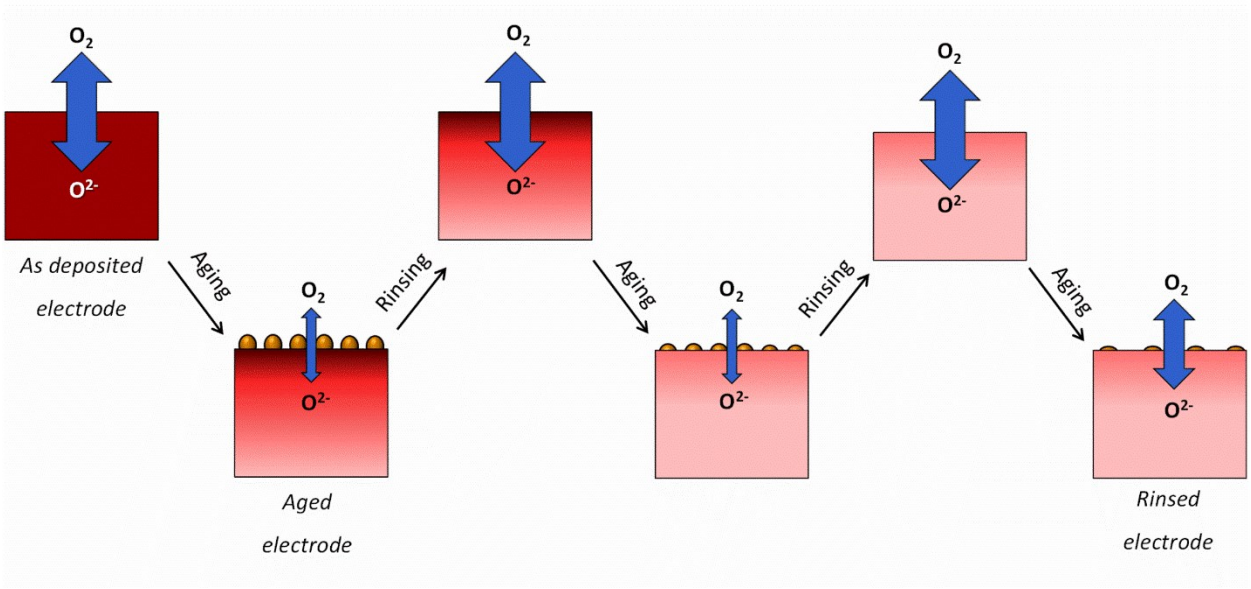

Figure 7. An illustration of the proposed passivation and activation mechanisms. During aging, strontium segregates to the surface and builds detrimental secondary phases. These phases are removed from the surface by rinsing in water, while the total amount of Sr in electrode gets depleted. After second rinsing, Sr amount in electrode is so much depleted (illustrated by lighter shades) that the driving force for Sr-segregation gets smaller which is then observed as slower degradation rate.

An important implication of these results is that earlier observed 'activated' and 'passive' states exist also in thin film electrodes at 600°C and below. The two states have markedly different oxygen exchange activities and a transition from passive to active can be realized by rinsing in water/acids. This fact can help to explain the significant scatter in oxygen exchange and ASR values reported in the literature. Since the 'passive' state is characterized by more stable, albeit low oxygen exchange activity, some studies have used the aged electrodes as a more reliable measure of oxygen exchange activity (e.g. Plonczak et al.[16]). On the other hand, in many other studies the reported values refer to 'fresh' electrodes measured shortly after the electrodes are heated to elevated temperatures, corresponding more to what we here refer to as 'activated' state. Moreover, this approach offers a simple way to recover the oxygen exchange activity in perovskite

View Article Online
DOI: 10.1039/D0CP02464C

oxides, which may be exploited to extend the life of oxygen electrodes in solid oxide cells and thereby reduce their operating costs.

5. Conclusion

The performance of thin $La_{0.6}Sr_{0.4}FeO_3$ electrodes was analyzed between 387° and 594°C and in pO_2 range from 1 to 0.05 bar. Area specific resistance was found to be strongly temperature-dependent with the apparent activation energy of ≈140 kJ/mol. A survey of similar thin film studies in the literature revealed huge discrepancies in the reported ASR and k_{chem} values. We offered an explanation for the observed differences in light of the existence of 'activated' and 'passive' states which appear the inevitable consequence of the sample's thermal history.

Electrochemical analysis coupled with the surface characterization of thin $La_{0.6}Sr_{0.4}FeO_3$ electrodes clarified further the passivation/activation mechanism on perovskite surfaces. The transition from the well-performing 'activated' state to the 'passive' state was shown to be correlated with the chemical state of strontium on the surface and related phase transformations. In addition to the cyclic nature of the phenomenon already discussed in our previous studies[5,6], we have here demonstrated that the once degraded, the electrodes can be reactivated and stabilized by a treatment in water.

Acknowledgements

Financial support by Danish innovation fund (Innovationsfonden) within the SYNFUEL project 4106-00006B is gratefully acknowledged. Authors would like to thank Yunzhong Chen for help with PLD.

Supporting Information.

Supporting Information for this work is available and contains the following sections:

View Article Online
DOI: 10.1039/D0CP02464C

- Testing setup
- XRD of deposited electrode
- SEM and film thickness
- Interpretation of impedance spectra
- Chemical capacitance
- Calculation of thermodynamic enhancement factor

Corresponding Author

*Đorđije Tripković, dordijetripkovic@gmail.com

Author Contributions

The manuscript was written through contributions of all authors. All authors have given approval to the final version of the manuscript.

Funding Sources

SYNFUEL project 4106-00006B

References

1 W. C. Chueh and S. M. Haile, *Annu. Rev. Chem. Biomol. Eng.*, 2012, **3**, 313–341.

2 M. Mosleh, M. Søgaard and P. V. Hendriksen, *J. Electrochem. Soc.*, 2009, **156**, B441.

3 S. B. Adler, J. A. Lane and B. C. H. Steele, *J. Electrochem. Soc.*, 1996, **143**, 3554.

4 J. Nielsen, T. Jacobsen and M. Wandel, *Electrochim. Acta*, 2011, **56**, 7963–7974.

5 Đ. Tripković, R. Küngas, M. B. Mogensen and P. V. Hendriksen, *J. Mater. Chem. A*, 2019, **7**, 11782–11791.

6 Đorđije Tripković, *PhD thesis*, Technical University of Denmark, 2018.

7 M. Kubicek, A. Limbeck, T. Frömling, H. Hutter and J. Fleig, *J. Electrochem. Soc.*, 2011, **158**, B727.

8 C. Graves, L. Martinez and B. R. Sudireddy , *ECS Trans.*, 2016, **72**, 183–192.

9 F. S. Baumann, J. Maier and J. Fleig, *Solid State Ionics*, 2008, **179**, 1198–1204.

10 S. B. Adler, *Solid State Ionics*, 1998, **111**, 125–134.

11 J. Januschewsky, M. Stöger-Pollach, F. Kubel, G. Friedbacher and J. Fleig, *Zeitschrift fur Phys. Chemie*, 2012, **226**, 889–899.

View Article Online
DOI: 10.1039/D0CP02464C

12 A. J. Darbandi and H. Hahn, *Solid State Ionics*, 2009, **180**, 1379–1387.

13 W. Ma, J. J. Kim, N. Tsvetkov, T. Daio, Y. Kuru, Z. Cai, Y. Chen, K. Sasaki, H. L. Tuller and B. Yildiz, *J. Mater. Chem. A*, 2015, **3**, 207–219.

14 E. J. J. Crumlin, E. Mutoro, S.-J. Ahn, G. J. la O', D. N. N. Leonard, A. Borisevich, M. D. D. Biegalski, H. M. M. Christen and Y. Shao-Horn, *J. Phys. Chem. Lett.*, 2010, **1**, 3149–3155.

15 J. Hayd, H. Yokokawa and E. Ivers-Tiffee, *J. Electrochem. Soc.*, 2013, **160**, F351–F359.

16 P. Plonczak, M. Søgaard, A. Bieberle-Hütter, P. V. Hendriksen and L. J. Gauckler, *J. Electrochem. Soc.*, 2012, **159**, B471–B482.

17 S. Pitscheider, *PhD Thesis*, Technical University of Denmark, 2018.

18 M. W. Den Otter, H. J. M. Bouwmeester, B. A. Boukamp and H. Verweij, *J. Electrochem. Soc.*, 2001, **148**, 1–6.

19 M. Søgaard, P. Vang Hendriksen and M. Mogensen, *J. Solid State Chem.*, 2007, **180**, 1489–1503.

20 M. Søgaard, A. Bieberle-Hütter, P. V. Hendriksen, M. Mogensen and H. L. Tuller, *J. Electroceramics*, 2011, **27**, 134–142.

21 J. E. ten Elshof, M. H. R. Lankhorst and H. J. M. Bouwmeester, *J. Electrochem. Soc.*, 1997, **144**, 1060.

22 Z. Cai, M. Kubicek, J. Fleig and B. Yildiz, *Chem. Mater.*, 2012, **24**, 1116–1127.

23 E. J. Crumlin, S.-J. Ahn, D. Lee, E. Mutoro, M. D. Biegalski, H. M. Christen and Y. Shao-Horn, *J. Electrochem. Soc.*, 2012, **159**, F219–F225.

24 A. Nenning, A. K. Opitz, C. Rameshan, R. Rameshan, R. Blume, M. Hävecker, A. Knop-Gericke, G. Rupprechter, B. Klötzer and J. Fleig, *J. Phys. Chem. C*, 2016, **120**, 1461–1471.

25 E. J. Crumlin, E. Mutoro, W. T. Hong, M. D. Biegalski, H. M. Christen, Z. Liu, H. Bluhm and Y. Shao-Horn, *J. Phys. Chem. C*, 2013, **117**, 16087–16094.

26 W. T. Hong, K. A. Stoerzinger, E. J. Crumlin, E. Mutoro, H. Jeen, H. N. Lee and Y. Shao-Horn, *Top. Catal.*, 2016, **59**, 574–582.

27 P. Hjalmarsson, M. Søgaard and M. Mogensen, *Solid State Ionics*, 2008, **179**, 1422–1426.

28 T. M. Huber, M. Kubicek, A. K. Opitz and J. Fleig, *J. Electrochem. Soc.*, 2014, **162**, F229–F242.

29 G. M. Rupp, A. Limbeck, M. Kubicek, A. Penn, M. Stöger-Pollach, G. Friedbacher and J. Fleig, *J. Mater. Chem. A*, 2014, **2**, 7099–7108.

30 G. M. Rupp, H. Téllez, J. Druce, A. Limbeck, T. Ishihara, J. Kilner and J. Fleig, *J. Mater. Chem. A*, 2015, **3**, 22759–22769.

31 E. Y. Konysheva and M. V. Kuznetsov, *RSC Adv.*, 2013, **3**, 14114.